

Reactivity of a di-Titanium Bis(pentalene) Complex towards Heteroallenes and Main Group Element–Element Bonds

Alexander F. R. Kilpatrick,[‡] Jennifer C. Green,[§] and F. Geoffrey N. Cloke.*[‡]

[‡] Department of Chemistry, School of Life Sciences, University of Sussex, Brighton, BN1 9QJ, United Kingdom

[§] Department of Chemistry, University of Oxford, Inorganic Chemistry Laboratory, South Parks Road, Oxford, OX1 3QR, United Kingdom

KEYWORDS titanium; metal-metal bonds; pentalene; homobimetallic; heteroallene; chalcogenide; imido

ABSTRACT: The reactivity of the Ti=Ti double bond in $(\mu:\eta^5, \eta^5\text{-Pn}^+)_2\text{Ti}_2$ (**1**), $\text{Pn}^+ = 1,4\text{-}\{\text{Si}^i\text{Pr}_3\}_2\text{C}_8\text{H}_4$ towards isocyanide and heteroallene substrates, and molecules featuring homonuclear bonds between main group elements (E–E) has been explored. Reaction of **1** with methylisocyanide or 1,3-*N,N'*-di-*p*-tolylcarbodiimide resulted in the formation of 1:1 adducts, $(\mu:\eta^5, \eta^5\text{-Pn}^+)_2\text{Ti}_2(\mu:\eta^2\text{-CNMe})$ (**2**) and $(\mu:\eta^5, \eta^5\text{-Pn}^+)_2\text{Ti}_2(\mu\text{-C}\{\text{N}(4\text{-C}_6\text{H}_4\text{CH}_3)\}_2)$ (**3**) respectively, which are thermally stable up to 100 °C in contrast to the analogous adducts formed with CO and CO₂. Reaction of **1** with phenylisocyanate afforded a paramagnetic complex, $[(\eta^8\text{-Pn}^+)\text{Ti}]_2(\mu\text{-}\kappa^2\text{-}\kappa^2\text{-O}_2\text{CNPh})$ (**4**), in which the ‘double-sandwich’ architecture of **1** has been broken and an unusual phenyl-carbonimidate ligand bridges two formally Ti(III) centers. Reaction of **1** with diphenyl dichalcogenides, Ph_2E_2 (E = S, Se and Te) led to a series of Ti–Ti single bonded complexes $(\mu:\eta^5, \eta^5\text{-Pn}^+)_2[\text{Ti}(\text{EPh})]_2$ E = S (**5**), Se (**6**) and Te (**7**), which can be considered the result of a 2e[−] redox reaction or a 1,2 addition across the Ti=Ti bond. Treatment of **1** with azobenzene or phenylazide afforded $[(\eta^8\text{-Pn}^+)\text{Ti}]_2(\mu\text{-NPh})_2$ (**8**), a bridging-imido complex in which the pentalene ligands bind in an η^8 -fashion to each formally Ti(IV) center, as the result of a 4e[−] redox reaction driven by the oxidative cleavage of the Ti=Ti double bond. The new complexes **2–8** were extensively characterized by various techniques including multinuclear NMR spectroscopy and single crystal X-ray diffraction, and the experimental work was complemented by density functional theory (DFT) studies.

INTRODUCTION

Interest in the chemistry of molecular compounds featuring bonds between transition metal atoms has rapidly increased over the past 50 years.¹ There are a growing number of reports of compounds in which group 4 metal atoms are directly bonded to late transition metals or p-block metals in heteronuclear di- and polynuclear complexes.^{2–4} Despite this, isolable compounds featuring a metal–metal bonding interaction between two group 4 metals are limited to a handful of examples.⁵

We have recently reported the synthesis and isolation of the dititanium bis(pentalene) complex $(\mu:\eta^5, \eta^5\text{-Pn}^+)_2\text{Ti}_2$ (**1**, $\text{Pn}^+ = 1,4\text{-}\{\text{Si}^i\text{Pr}_3\}_2\text{C}_8\text{H}_4$),⁶ which density functional theory (DFT) studies revealed to have two metal–metal bonds and a low lying metal-based empty orbital. Complex **1** shows unprecedented reactivity amongst other known di-metal ‘double sandwich’ complexes,^{7–12} including multiple adduct formation with carbon monoxide and reductive activation of carbon dioxide.¹³ In the case of CO₂ mechanistic studies have shown that an adduct is formed with **1** at low temperatures, which reacts further upon warming to RT. Furthermore, we have managed to model this thermally unstable CO₂ adduct by the reaction of **1** with its sulfur congener, CS₂.¹⁴

The reactivity of **1** towards CO and CO₂ encouraged us to examine its reactivity towards related organic substrates, in isocyanides, carbodiimides and isocyanates, and also toward organic substrates containing main group elements (E). Our aims were to form new adducts of the di-metal double-sandwich motif and explore the scope for multi-electron redox reactions across the Ti=Ti double bond.

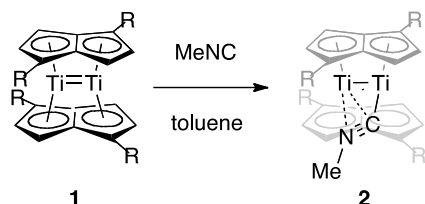
RESULTS AND DISCUSSION

Isocyanides

Organic isocyanides (RN≡C:) are isolobal with carbon monoxide, and have shown interesting reactivity with low-valent transition metals and M–M bonded complexes to complement that of CO.¹⁵ Treatment of a solution of **1** in toluene-*d*₈ with two equivalents of MeNC resulted in a purple reaction mixture, the ¹H NMR spectrum of which showed eight doublets in the aromatic region, similar to that of monocarbonyl adduct $(\mu:\eta^5, \eta^5\text{-Pn}^+)_2\text{Ti}_2(\mu:\eta^2\text{-CO})$.¹⁴ A ¹H NMR resonance at 3.25 ppm was assigned to the methyl group of coordinated MeNC, in *ca.* equal ratio to the one at 1.18 ppm assignable to the free isocyanide. The ¹³C{¹H} spectrum displayed 16 aromatic signals, while a signal at δ_{C} 289 ppm (shifted downfield from δ_{C} 158 ppm for free MeNC)¹⁶ was also observed. Furthermore the

$^{29}\text{Si}\{^1\text{H}\}$ NMR spectrum consisted of 4 signals at δ_{Si} 7.92, 7.26, 7.23 and 6.25 ppm. These spectroscopic observations are consistent with a 1:1 adduct formation (**2**) where the C_2 molecular symmetry of **1** has been broken (Scheme 1).

Scheme 1. Synthesis of methylisocyanide adduct 2. R = Si^iPr_3 .



This is in contrast to the reactivity of **1** with CO, where ligation of more than one CO is observed under an overpressure of the gas, and is attributed to steric congestion.¹⁷ The solution structure of **2** was confirmed in the solid state by a single crystal X-ray diffraction (XRD) study, revealing a $\mu\text{-CNMe}$ ligand asymmetrically bridging the Ti_2 core (Figure 1).

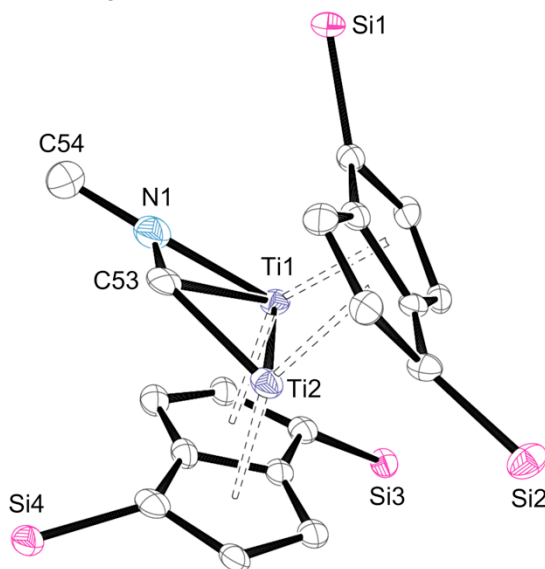


Figure 1. ORTEP plot of **2**. H atoms and $i\text{Pr}$ groups omitted for clarity. 30% ellipsoids.

Table 1 Selected distances (\AA), angles ($^\circ$) and parameters (defined in Chart 1) for molecular structure **2** determined by X-ray crystallography and optimized structure **II** calculated by DFT.

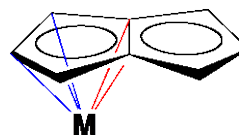
Parameter	2	II
Ti–Ti	2.4120(15)	2.400
C53–Ti _{proximal}	2.016(6)	2.051
C53–Ti _{distal}	2.326(7)	2.246
N1–Ti _{distal}	2.147(6)	2.148
C53–N1	1.219(10)	1.262
Ti–Ct ^a	2.080(2)	2.083
Ct–Ti–Ct ^a	142.94(11)	141.74

Ti–C53–N1	133.3(6)	136.80
Δ ^a	0.103	0.091
TA	17.5(4)	0.11

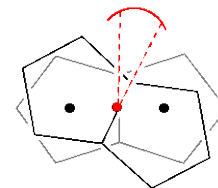
^aAverage values. Ct denotes the η^5 -centroid of a Pn ring.

Chart 1. Definition of the geometric parameters Δ and TA.

Ring slippage (Δ)



Twist angle (TA)



$$\Delta = \Sigma(\text{M-C}_{\text{bridge}})/2 - \Sigma(\text{M-C}_{\text{wing}})/3$$

Comparison of the solid-state structure of **2** with the previously reported side-on monocarbonyl adduct,¹⁴ reveals slightly longer Ti–Ti and Ti–C53 distances in the former complex. However **2** shows a closer approach of the MeNC-nitrogen atom to the distal Ti atom compared with that of the CO-oxygen atom in $\text{Ti}_2(\mu:\eta^5, \eta^5\text{-Pn}^+)_2(\mu:\eta^2\text{-CO})$, consistent with the relative availability of the N lone pair in valence bond structure for isocyanides,⁸ compared with the predominantly zwitterionic valence bond character of CO.¹⁹ This is reflected in a more acute angle Ti–C–E about the semi-bridging carbon atom in **2** ($138.4(6)^\circ$, E=N) compared with $(\mu:\eta^5, \eta^5\text{-Pn}^+)_2\text{Ti}_2(\mu:\eta^2\text{-CO})$ ($146.4(13)^\circ$, E=O). However, the low quality of the X-ray data for **2** warrants a degree of caution with regard to this interpretation. The structural parameters (Chart 1) for $\text{Pn}_2\text{Ti}_2(\mu:\eta^2\text{-CNMe})$ (**II**) calculated using DFT at the BP86 level of theory (Table 1) are in reasonable agreement with the experimental values for **2**, and are in keeping with the comparison with the mono-CO complex, showing slightly longer Ti–Ti, C–Ti_{proximal} and C–O/N distances and a stronger interaction between the MeNC-nitrogen atom to the distal Ti atom in **II** compared with that of the CO-oxygen atom in $\text{Pn}_2\text{Ti}_2(\mu:\eta^2\text{-CO})$.¹⁷

The IR spectrum of **2** shows a $\nu(\text{CN})$ stretch at 1642 cm^{-1} , an unusually low value for bridging isocyanide ligands in bimetallic complexes, which typically range from 1700 to 1870 cm^{-1} .²⁰ However, bridging isocyanide adducts of M–M bonded tungsten alkoxide dimers reported by Chisholm *et al.* also show very low $\nu(\text{CN})$ values (*ca.* 1530 cm^{-1}),²¹ which has been attributed to increased back bonding from the metal d-orbitals to the vacant high-energy π^* -orbitals of the isocyanide ligand. The calculated $\nu(\text{CN})$ wavenumber for **II** is 1638 cm^{-1} , in good agreement with the experimental value. Inspection of the frontier MOs (Figure S5) indicates there is significant back-donation from the HOMO of the Ti_2Pn_2 fragment which steers the MeNC ligand to a side-on position, as was found for the monocarbonyl adduct.¹⁴

The formation of a 1:1 methylisocyanide adduct **2**, which persists in the presence of excess MeNC, is in marked contrast to the higher adducts formed by reaction of **1**

with 2 or 3 equivalents of CO. This encouraged us to investigate the chemistry of **1** with nitrogen containing heteroallenes, with the aim of forming adducts which are more thermally stable than that found with CO₂.

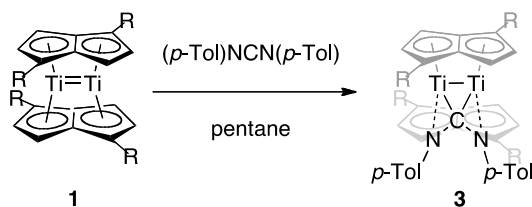
Reactivity with Heteroallenes

Carbodiimides

Heteroallenes, of general formula X=Y=Z where at least one of the functional atoms X, Y or Z is a heteroatom (in most cases N, O or S) are commonly used to model the reactivity of CO₂.²² However, reactivity of heteroallenes is strongly influenced by the electronic effects of the attached substituents,²³ and carbodiimides (X = Z = NR, Y = C) have shown particularly varied chemistry with low valent titanium complexes.^{24,25}

Addition of one equivalent of 1,3-*N,N'*-di-*p*-tolylcarbodiimide (*p*-TCD) to a solution of **1** in pentane resulted in a color change to brown-green. Subsequent work-up and recrystallization from SiMe₄ afforded bronze crystals in excellent yield (92%), which were identified by analytical and spectroscopic methods as compound **3** (Scheme 2).

Scheme 2. Synthesis of carbodiimide adduct 3. R = Si^{*i*}Pr₃.



In more detail the mass spectrum showed a complex mass envelope in the region 1144–1149 amu and an isotopic pattern consistent with the formulation of a 1:1 adduct depicted in Scheme 2. Furthermore, the ¹H NMR spectrum of **3** displays four sharp doublets in the aromatic region assigned to the Pn⁺ ring protons (Figure S1), consistent with a C₂-symmetric structure in solution. The ¹³C{¹H} spectrum displayed 12 signals in the aromatic region assignable to the ligand scaffold (8 for pentalene and 4 for the *p*-tolyl) while a signal at 182.3 ppm was assigned to the carbodiimide central carbon atom (Figure S2). NMR spectral assignments were verified by recourse to 2D ¹H–¹³C correlation experiments (Figures S3 and S4).

Single crystal X-ray diffraction studies unambiguously confirmed the molecular structure of **3** in the solid state, which agrees with solution NMR spectroscopic data. The molecular structure (Figure 2) shows a bent *p*-TCD ligand in a μ:η²,η²- binding mode between two Ti centers forming a dimetalocyclopropane-type motif with a Ti–C–Ti angle of 68.2(2)°. In a similar fashion to the related mono(oxo) complex, (μ:η⁵,η⁵-Pn⁺)₂Ti₂(μ-O),¹⁴ **3** possesses a S₂ axis passing through the carbodiimide carbon (C53) and the midpoint of the Ti–Ti bond, which results in one half of the dimer being generated by symmetry.

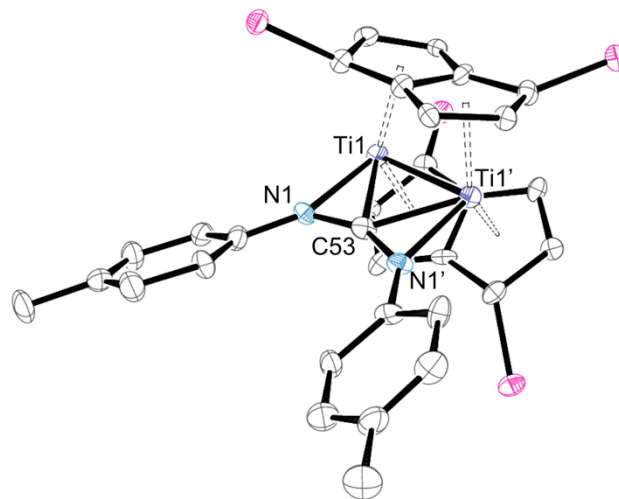


Figure 2. ORTEP (30% probability) diagram of **3**. H atoms and *i*Pr groups omitted for clarity. Primed atoms are generated by symmetry ($-x, y, -z+3/2$). Selected distances (Å), angles (°) and parameters: Ti1–Ti1' 2.4374(8), Ti1–C53 2.176(2), Ti1–N1 2.1159(15), C53–N1 1.3004(15), Ti–Ct^a 2.1218, Δ^a 0.034(2), Pn C–C_{ring}^a 1.459(3), *p*-Tol C–C_{ring}^a 1.390(3); Ti1–C53–Ti1' 68.13(7), C53–Ti1–Ti1' 55.94(4), Ti1–C53–N1 69.87(9), N1–C53–N1' 152.2(2), Ct1–Ti1–Ct2 137.83(4), TA 22.5(3). Ct denotes the η²-centroid of the Pn ring. ^aAverage values.

The distance of each Ti atom **3** from the central carbon atom of the carbodiimide is 2.176(2) Å, in the range of a Ti–C single bond ($\Sigma r_{\text{cov}} = 2.11$ Å),²⁶ and comparable to that found in Rosenthal's carbene-like dinuclear Ti(III) complex,

[Cp₂Ti(μ-κ²:η¹-{Cy}NCN{Cy})TiCp₂], (2.199(4) Å).²⁷ Indeed, the Ti–C distance in **3** is comparable with the shorter Ti–C_{carbene} distances of titanium complexes with NHC ligands reported to date, which range from 2.160(3)²⁸ to 2.212 Å,²⁹ however, it is significantly longer than those for Schrock-type titanium carbene complexes (ca. 1.830 Å).³⁰ The Ti–N distance in **3** (2.1159(15) Å), while in the range of a Ti–N single bond ($\Sigma r_{\text{cov}} = 2.07$ Å),²⁶ is notably longer than those of titanocene(III) amides such as Cp⁺₂Ti(NRH) (1.9555(5) Å R = Me,³¹ 1.944(2) Å R = H,³²) as these complexes have an additional π-bonding interaction from the N lone pair. However, this value is shorter than in Cp⁺₂Ti(NMePh) (2.157(5) Å),³³ where the Ti–amide bond lacks its π-constituent due to steric congestion. The metrics of the TiNC unit in **3** are best compared with those found in monomeric titanocene(III) η²-aminoacyl complexes, for example Cp₂Ti(η²-{Ph}CN{Xyl})³⁴ and [Cp₂Ti(η²-{Me}CN{^{*i*}Bu})][BPh₄] (Ti–C = 2.096(4) and 2.080(6) Å; Ti–N = 2.149(7) and 2.125(5) Å respectively). Complex **3** features a more acute Ti–C–N angle (69.87(9)°) than in these η²-aminoacyl complexes presumably due to further conjugation at the carbodiimide central carbon atom to the second half of the dimer. The carbodiimide moiety in **3** is bent with a N–C–N angle of 152.2(2)° and the C–N bond lengths of 1.3004(15) Å are consistent with the partial loss of the cumulene structure of the free substrate upon

complexation. For comparison, in the free carbodiimide, the N=C=N angle is 170.4(4)° and the C–N bond lengths are 1.223(5) and 1.204(4) Å.³⁵ This is further reflected in the IR spectrum which shows a $\nu(\text{NCN})$ asymmetric stretching vibration at 1659 cm⁻¹, a value significantly lower than that of *p*-TCD ($\nu_{\text{NCN}} = 2139$ cm⁻¹).³⁶ The molecular structure of **3** is reminiscent of carbodiimide adducts of M–M bonded di-tungsten complexes W₂(O^{*i*}Bu)₆ and W₂(OCMe₂CF₃), which have been structurally characterized.^{37,38}

Compound **3** is thermally robust, with no change observed by ¹H NMR spectroscopy after heating at 100 °C in methylcyclohexane-*d*₁₄ for 4 days. This may be attributed to the kinetic stability imparted on the carbenic carbon atom, which is a potential reactive site, but is somewhat buried in the ‘cleft’ provided by the Ti₂ double-sandwich structure and the *p*-tolyl substituents of the carbodiimide.

Isocyanates

Organic isocyanates, RN=C=O, have also been studied as reagents for modeling the reactivity of CO₂, since the introduction of an amido (RN) group results in polarization of the double bonds and thus increased reactivity.³⁹ Slow addition of PhNCO to a pentane solution of **1** at –35 °C resulted in a green-brown solution upon warming to room temperature, which after concentration and cooling to –35 °C, deposited green single crystals suitable for X-ray diffraction analysis. The molecular structure (Figure 3) revealed not the anticipated PhNCO adduct but complex **4** in which the double-sandwich structure has been cleaved and an unusual phenyl-carbonimidate ligand bridges two formally Ti(III) centers. Complex **4** was further characterized by mass spectrometry, elemental analysis and IR spectroscopy. The ¹H NMR spectrum of **4** in THF-*d*₈ displays only broad signals, and the effective magnetic moment determined by the Evans method was 1.3 μ_B per Ti, which is less than the spin-only value for a Ti³⁺ ion (1.73 μ_B).

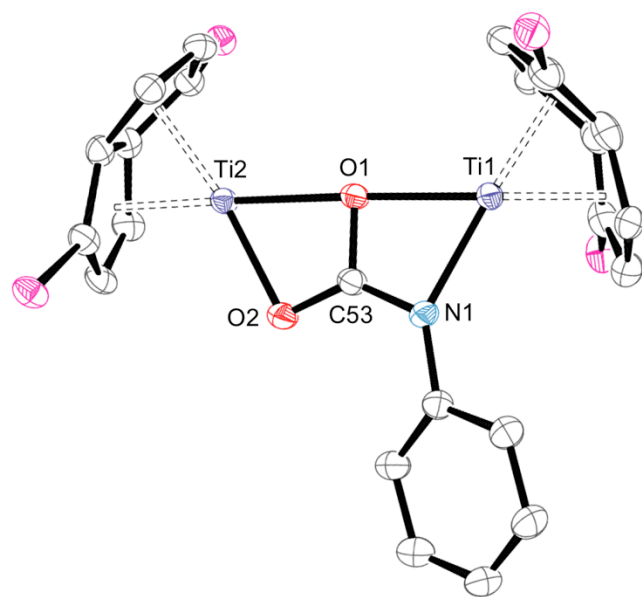


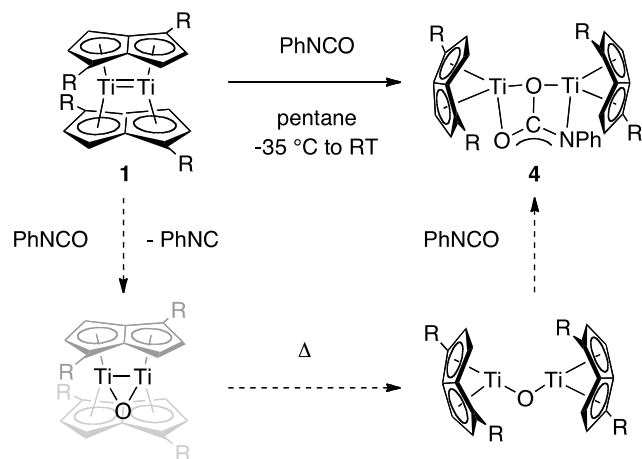
Figure 3. ORTEP (30% probability) diagram of **4**. H atoms and ⁱPr groups omitted. Selected distances (Å) and angles (°): Ti1–Ti2 4.3011(11), Ti1–O1 2.145(2), Ti2–O1 2.146(2), Ti1–N1 2.124(3), Ti2–O2 2.081(3), C53–O1 1.350(4), C53–O2 1.275(4), C53–N1 1.314(4), Ti–Ct^a 1.9354(18); Ti1–O1–Ti2 176.44(12), O1–Ti1–N1 62.90(9), O1–Ti2–O2 63.10(9), O1–C53–N1 113.4(3), O1–C53–O2 114.8(3), O2–C53–N1 131.7(3), Ct–Ti–Ct^a 57.32(9), Fold angle 35.1(3). Ct denotes the η⁵-centroid of the Pn ring.^a Average values.

The bond distances about the central carbon atom of the bridging ligand are between the range for a C(sp²)–E single and double bond (C–O: 1.293–1.407; C=O: 1.187–1.255; C–N: 1.279–1.329; C=N: 1.321–1.416 Å).^{40,41} The ‘NCO[–]’ core is planar and the sum of its angles is 360°. These data imply the delocalization of negative charge over the bidentate phenyl-carbonimidate ligand. Other examples of this ligand in the Cambridge Structural Database (CSD) are limited to a single report by Zhou and co-workers⁴² which details a series of lanthanide(III) complexes, [Cp₂Ln(THF)]₂(μ-κ²:κ²-O₂CNPh) (Ln = Y, Er, Yb), showing similar metrics about the [PhNCO₂]^{2–} bridge. These complexes were prepared from the lanthanocene(III) hydroxides [Cp₂Ln(μ-OH)(THF)]₂ and PhNCO followed by reaction with the corresponding Cp₃Ln. In contrast a redox reaction has clearly taken place between **1** and PhNCO to afford **4**.

The yield was 40% with respect to **1** and PhNCO, however, based on the formula of **4** with two oxygens atoms in the bimetallic product, the reaction stoichiometry requires two equivalents of PhNCO per dimer. Reaction of **1** in methylcyclohexane-*d*₁₄ with 1 equiv of PhNCO showed a mixture of products by ¹H NMR spectroscopy, including resonances assignable to mono(μ-oxo) complex (μ:η⁵,η⁵-Pn⁺)₂Ti₂(μ-O) and free PhNC. The analogous reaction using 2 equiv of PhNCO produced a complex ¹H NMR spectrum, indicating a mixture of diamagnetic and paramagnetic components that could not be assigned.

The mechanism for this unexpected transformation is as yet unclear, but it can be postulated to proceed *via* O-atom transfer from PhNCO to give (μ:η⁵,η⁵-Pn⁺)₂Ti₂(μ-O) (Scheme 3), which is known to be thermally unstable with respect to the more open triplet structure [(η⁸-Pn⁺)Ti]₂(μ-O).¹⁴ The third step involves nucleophilic attack of the μ-O ligand at the carbon atom of a second PhNCO molecule, a position which is generally nucleophilic.⁴³ It is noteworthy that the reaction **1** with PhNCO is kinetically stabilized at a carbonimidate-bridged Ti(III)–Ti(III) complex, in contrast to the heteroallenes CO₂ and COS which give oxo- and sulfido-bridged Ti(IV)–Ti(IV) products respectively.¹⁴

Scheme 3. Synthetic route to **4** (R = Si^{*i*}Pr₃), *via* postulated intermediates.



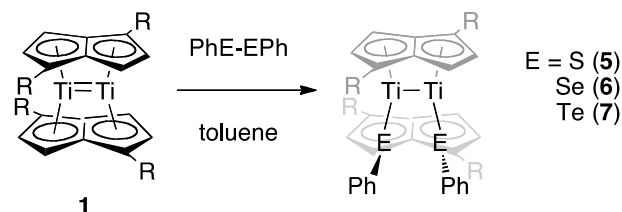
Reactivity with Main Group Element–Element Bonds

Diphenyl dichalcogenides

Organic dichalcogenides, RE–ER (E = S, Se, Te; R = alkyl or aryl), are commonly employed as redox active substrates with low valent metal complexes including those of early transition metals.^{44,45} With highly reducing metal complexes E–E bond cleavage of the dichalcogenide routinely occurs to yield a complex bearing the respective chalcogenoate (RE)[−] ligands.

When deep red solutions of **1** in toluene were treated with one equivalent of Ph₂E₂ (E = S, Se and Te) an immediate color change from deep red to red-brown was observed. Subsequent work-up and recrystallization from pentane furnished the respective di-phenylchalcogenoate complexes (μ:η⁵,η⁵-Pn⁺)₂[Ti(EPh)]₂, for E = S (**5**), Se (**6**) and Te (**7**) as analytically pure brown solids (Scheme 4).

Scheme 4. Synthesis of di-phenylchalcogenoate complexes 5–7. R = SiⁱPr₃.



EI-MS showed a parent ion or a common fragment ([M – Ph]⁺ or [M – ⁱPr]⁺) for each complex. Solid state IR for **6** and **7** showed essentially identical spectra with a sharp band at ca. 1570 cm^{−1} assigned to the aromatic C=C stretch of the phenyl group. In contrast **5** shows a broad IR band at 1620 cm^{−1}. ¹H NMR spectroscopy showed very similar spectra for **5**, **6** and **7**, consisting of seven sharp signals in the aromatic region; three of which were assigned to the *o*, *m*, and *p*-H of the two equivalent Ph groups with integration and multiplicity as expected; four doublet signals

of equal intensity were assigned to the Pn⁺ ring protons in a double-sandwich structure with C₂ symmetry on the NMR timescale. Multinuclear (¹³C, ²⁹Si) NMR spectra were consistent with this interpretation. The ⁷⁷Se{¹H} and ¹²⁵Te{¹H} NMR of **6** and **7** respectively showed one singlet signal at δ_{Se} 511 and δ_{Te} 418 respectively. These chemical shifts are relatively lower in frequency in comparison with those of known titanium selenolate and telluroate complexes, for which ⁷⁷Se{¹H} and ¹²⁵Te{¹H} NMR spectroscopic data are shown in Table 2. This may be correlated with the formally Ti(III)–Ti(III) oxidation state in **6** and **7**, which renders the chalcogenoate ligand more shielded with respect to monomeric d⁰ Ti(IV) complexes. However, the (RE)[−] ligands in these literature examples have very different electronic properties, so firm comparisons cannot be made. Known Ti(III) selenolate and telluroates such as Cp₂Ti^{III}[TeSi(SiMe₃)₃]PMe₃⁴⁶ precluded NMR characterization due to their paramagnetic nature.

The (Pn⁺)₂Ti₂ double-sandwich motif can incorporate both terminal and bridging ligands, and titanium thiolates complexes with terminal and bridging bonding modes are well known.⁴⁷ Spectroscopic and analytical data alone were not sufficient to distinguish between a terminal or bridging mode for the chalcogenolate ligands, so a single crystal XRD study was carried out.

Table 2. Solution ⁷⁷Se{¹H} and ¹²⁵Te{¹H} NMR data for **6, **7** and related Ti selenolate and telluroate complexes.**

Compound	δ	solvent	ref
6	511	cyclohexane- d ₁₂	this work
Cp ₂ Ti(<u>Se</u> Ph) ₂	847	n/a	48
Cp ₂ Ti(<i>o</i> - <u>Se</u> ₂ C ₆ H ₄)	982	n/a	48
Cp ₂ Ti(<u>Se</u> Me) ₂	914.2	CD ₂ Cl ₂ /CH ₂ Cl ₂	49
Ti[<u>Se</u> Si(SiMe ₃) ₃] ₄	865	C ₆ D ₆	50
Ti[<u>Se</u> Si(SiMe ₃) ₃] ₃ CH ₂ P	828	C ₆ D ₆	50
Ti[<u>Se</u> Si(SiMe ₃) ₃] ₂ (OEt)	416	C ₆ D ₆	50
7	418	cyclohexane- d ₁₂	this work
Cp ₂ Ti[<u>Te</u> Si(SiMe ₃) ₃] ₂	810	C ₆ D ₆	51
Cp ^{Me} ₂ Ti[<u>Te</u> Si(SiMe ₃) ₃] ₂	783	C ₆ D ₆	51
Cp ₂ Ti(<u>Te</u> SiPh ₃) ₂	709	C ₆ D ₆	52
Cp ^{Me} ₂ Ti(<u>Te</u> SiPh ₃) ₂	659	C ₆ D ₆	52

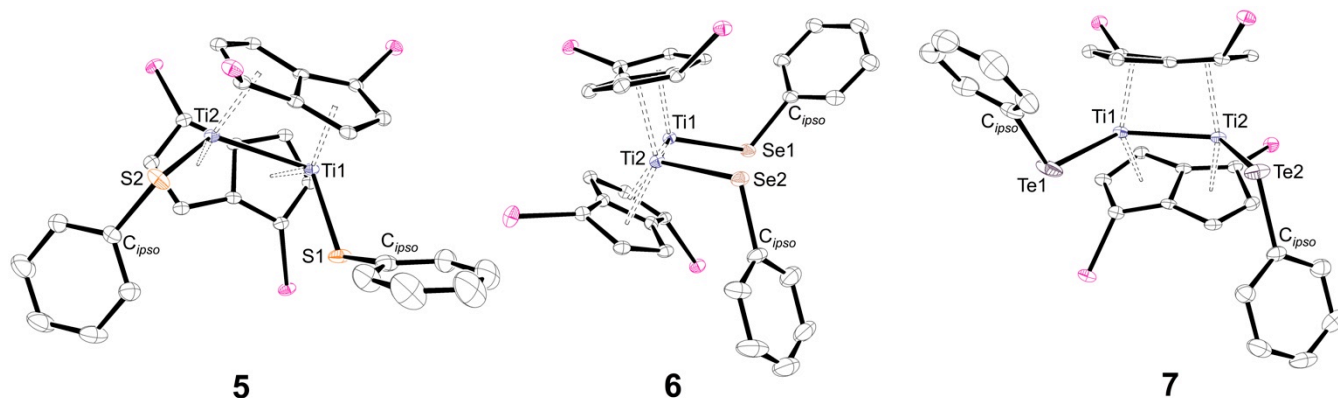


Figure 4. ORTEP plots of (left to right) 5, 6 and 7. H atoms and *i*Pr groups omitted for clarity. 30% ellipsoids.

Table 3. Selected distances (Å), angles (°) and parameters for 1,⁶ 5, 6 and 7.

Parameter	1 ⁶	5	6	7
Ti1–Ti2	2.399(2)	2.6519(9)	2.6581(15)	2.6530(9)
Ti–E ^a	-	2.3477(11)	2.4769(13)	2.6866(7)
Ti–Ct ^a	2.036(4)	2.0875(19)	2.0874(11)	2.0807(17)
Ti–C _{ring} ^a	2.378(7)	2.416(3)	2.416(6)	2.411(4)
Δ ^a	0.005(7)	0.130(3)	0.120(6)	0.115(4)
Pn C–C _{ring} ^a	1.449(5)	1.431(2)	1.437(9)	1.438(2)
Ph C–C _{ring} ^a	-	1.381(4)	1.384(14)	1.384(4)
Ti–Ti–E ^a	-	118.58(4)	119.30(6)	120.69(3)
Ti–E–C _{ipso} ^a	-	118.27(15)	115.0(2)	112.65(13)
C _{ipso} –E–E–C _{ipso}	-	120.5(2)	127.6(3)	140.73(18)
E–Ti–Ti–E	-	15.26(7)	13.19(8)	7.01(5)
Ct–Ti–Ct ^a	155.22(19)	133.92(7)	134.35(6)	135.14(7)
TA	20.1(8)	21.6(3)	19.1(5)	17.4(3)

^aAverage values. Ct denotes the η⁵-centroid of a Pn ring.

Et₂O solutions of the respective thiolate and selenolate complexes **5** and **6**, and a SiMe₄ solution of telluroate complex **7**, each provided single crystals which were of sufficient quality for structural determination by XRD. The general structural feature common to **5**, **6** and **7** is the double-sandwich motif with terminal di-chalcogenoate ligands pointing out of one face, and the Ph groups pointing in opposite directions to minimize steric repulsions with the Si^{*i*}Pr₃ substituents on this face. The molecular structures of **5**, **6** and **7** are depicted in Figure 4 and selected structural parameters are compared in Table 3.

The most noteworthy structural feature is the longer Ti–Ti distance for **7** (2.6530(9) Å) with respect to the starting compound **1** (2.399(2) Å),⁶ consistent with the loss of two electrons from the M–M bonding HOMO of **1** upon oxidative addition of Ph₂Te₂. Indeed, the intermetallic distance is significantly longer than in the mono(chalcogenide) complexes Ti₂(μ:η⁵,η⁵-Pn⁺)₂(μ-O) and Ti₂(μ:η⁵,η⁵-Pn⁺)₂(μ-S) (2.3991(7) and 2.4682(8) Å respectively),¹⁴ and Cummins' (tri-*tert*-butylsilyl)imido complex [(^{*t*}Bu₃SiNH)Ti]₂(μ-NSi^{*t*}Bu)₂ (2.442(1) Å).⁵³

The Ti–Te distances for **7** (av. 2.6866(7) Å) lie between the sum of their single and double bond covalent radii (2.72 and 2.45 Å respectively),⁵⁴ and are comparatively short relative to those of previously determined telluroate complexes of Ti(III), Cp₂Ti[TeSi(SiMe₃)₃]PMe₃ (2.8955(30) Å), Cp₂Ti(TeSnPh₃) (2.8681(18) Å)⁵¹ and even of Ti(IV), Cp₂Ti[TeSi(SiMe₃)₃]₂ (2.788(1) Å).⁵¹ This suggests a possible π-bonding interaction between titanium and tellurium in **7**, an effect which has been invoked in the permethyltitanocene(III) telluride complex [Cp*₂Ti]₂(μ-Te),⁵⁵ which shows an average Ti–Te distance of 2.702(3) Å. The angle between the Ti–Te vectors (61.7°) reflects the extent to which the large Te atoms are pointing away from each other, in contrast to the dicarbonyl complex (μ:η³,η⁵-Pn⁺)₂[Ti(CO)]₂ in which the Ti–C_{CO} vectors are near parallel (9.8°).¹³

DFT geometry optimizations (BP86/TZP) were carried out on model complexes Pn₂Ti₂(EPh)₂ (E = S, Se, Te) with no symmetry constraints and gave structures with C₂ symmetry. Selected metric parameters are listed in Table 4.

Table 4. Selected distances (Å), angles (°) and parameters for DFT optimized structures $\text{Pn}_2\text{Ti}_2(\text{EPh})_2$ (E = S, Se, Te).

Parameter	S	Se	Te
Ti–Ti	2.631	2.606	2.606
Ti–E ^a	2.389	2.521	2.729
Ti–Ti–E ^a	118.1	113.7	115.0
Ti–E–C _{ipso} ^a	116.8	113.7	111.3
E–Ti–Ti–E	13.44	13.93	11.59

^aAverage values

The tellurolate complex $\text{Pn}_2\text{Ti}_2(\text{TePh})_2$ was selected for fragment analysis as the Te orbitals were most separated from the π -orbitals of the Ph ring. The molecule was split into Pn_2Ti_2 and TePh fragments in the computed geometry of the molecule (see ref. 6 and Table S3 for the fragment orbitals of Pn_2Ti_2 and TePh respectively). Considering the Pn_2Ti_2 fragment, the HOMO (Figure 5) shows the Ti–Ti σ -bond remains intact and the other frontier MOs are all partially populated (see Supporting Information Table S2), presumably to maximize bonding to the EPh groups. The chalcogenolate ligands each use two $p\pi$ -orbitals to bind to titanium; the HOMO–3 (Figure 5) shows a Ti–Te σ -bond formed largely by the $p\pi$ -orbital perpendicular to the Ph ring (MO 23 in Figure S6), and the HOMO–4 and –5 show a π -type interaction between Ti and the $p\pi$ -orbital parallel to the Ph ring (MO 22 in Figure S6). The HOMO–1 (Figure 5) shows Te π -orbitals pointing towards each other and out of phase, which could explain the relatively large Te–Ti–Ti–Te torsion angle found for 7.

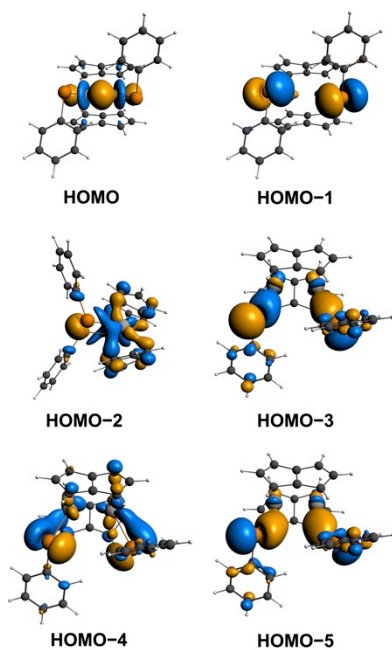


Figure 5. Isosurfaces for the key Ti–Te bonding MOs of $\text{Pn}_2\text{Ti}_2(\text{TePh})_2$.

Terminal chalcogenolate ligands act as one electron donors (X-function in the CBC method)⁵⁶ meaning 5, 6 and 7 are formally 17 valence electron (VE) per Ti, with diamagnetic behavior which may be explained by a M–M single bond. This prompted us to investigate the potential for a 4e[−] oxidation of 1 to give 18 VE per Ti center, and the effect this would have on the double-sandwich structure. Azobenzene was selected as a substrate, given its ability to undergo both 2e[−] and 4e[−] redox reactions with low valent metal complexes.

Azobenzene and phenylazide

The redox chemistry of azobenzene, $\text{PhN}=\text{NPh}$, with low-valent metal complexes has been widely studied.⁵⁷ Floriani *et al.* reported the synthesis of a *cis*-azobenzene adduct of titanocene, $\text{Cp}_2\text{Ti}(\eta^2\text{-N}_2\text{Ph}_2)$, by the reaction of $\text{Cp}_2\text{Ti}(\text{CO})_2$ with Ph_2N_2 .^{58,59} Subsequent *ab initio* MO calculations suggest this diamagnetic complex is best described as a 1,2-diphenylhydrazido(2−) ligand and a formally Ti(IV) center.⁶⁰ Recent work by Beckhaus *et al.* has utilized this preference for *cis*-azo ligation to titanocene fragments to synthesize supramolecular squares.⁶¹ There are also several examples of azobenzene reduction and cleavage leading to terminal phenylimido complexes in Ti chemistry,^{62–66} which constitutes a four-electron process per azobenzene.

Addition of one equivalent of azobenzene to a toluene solution of 1 resulted in a color change to dark red. Removal of the solvent and recrystallization from hexane furnished red crystals of $[(\eta^8\text{-Pn}^+)\text{Ti}]_2(\mu\text{-NPh})_2$ (8), isolated in 70% yield (Scheme 5). Elemental analysis and EI-MS data support the proposed formulation. Solution phase NMR spectroscopy data are consistent with a C_{2v} symmetric structure; the ¹H spectrum contains two signals assigned to the Pn^+ ring protons and three further signals in the aromatic region assigned to the two equivalent Ph groups.

X-ray diffraction analysis of single crystals of 8 revealed two phenylimido ligands bridging two formally Ti(IV) centers, forming a Ti_2N_2 heterocyclic ring (Figure 6). The coordination geometry of both titanium atoms is distorted tetrahedral, and the intermetallic distance (2.8935(5) Å) is not unusually short for a di-Ti(IV) complex, and similar distances have been observed in related species.^{67–70} The bridging region of the complex is asymmetric, such that the Ti–N bond lengths are different, ranging from 1.9830(17) Å to 1.9536(17) Å. Asymmetrically bridging imido ligands have previously been observed for several different transition-metal complexes, and Nugent *et al.* have ascribed this effect to an increase in π -donation to the metal center.⁷⁰ However, these researchers suggested that a substantial distortion of the M–N bond lengths in four-coordinate group 4 $[\text{M}_2(\mu\text{-NR})_2]$ -containing complexes is not expected on electronic grounds. Hence, it is postulated that the difference in the Ti–N bond lengths in 8 is sterically induced by the asymmetric disposition of the Pn^+ ligands with respect to the $[\text{Ti}_2(\mu\text{-NPh})_2]$ unit. The

reaction can be considered a 4e⁻ reduction per azobenzene molecule driven by the oxidative cleavage of the Ti=Ti double bond.

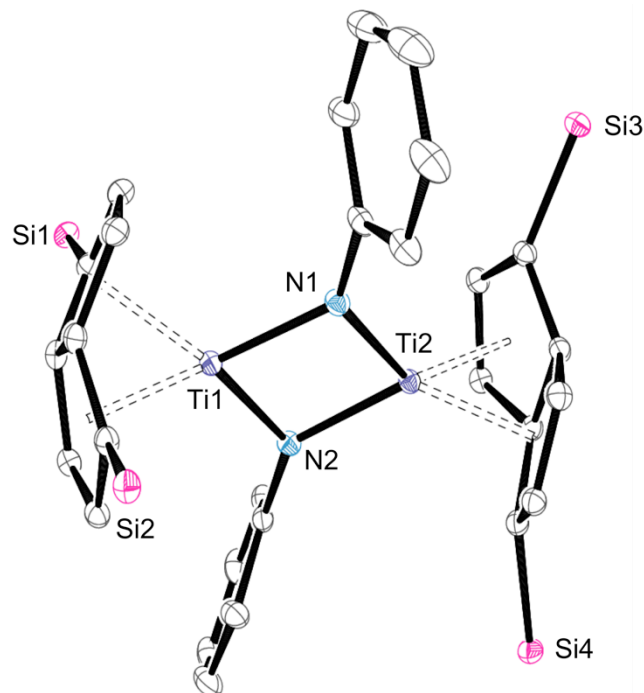
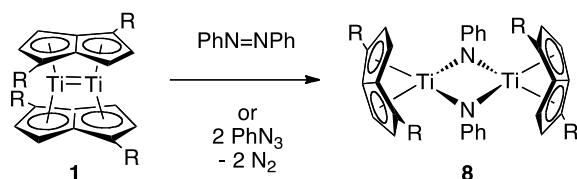


Figure 6. ORTEP (30% probability) diagram of **8**. H atoms and ⁱPr groups omitted for clarity. Selected interatomic distances (Å) and angles (°): Ti1–Ti2 2.8935(5), Ti1–N1 1.9799(17), Ti1–N2 1.9614(17), Ti2–N1 1.9536(17), Ti2–N2 1.9536(17), Ti–Ct^a 1.9975(10), Pn C–C_{ring}^a 1.443(3), Ph C–C_{ring}^a 1.401(3); Ti1–N1–Ti2 94.47(7), Ti1–N1–Ti2 94.61(7), Ct–Ti–Ct^a 56.57(4), TA 32.30(15), Fold angle 32.6(3). ^a Average values.

Organic azides (RN₃) are common reagents for the transfer of an imido (RN) group to a metal complex, upon loss of N₂, and presented an alternative synthetic route to **8**. Addition of 1 equivalent of azidobenzene (PhN₃) to a solution of **1** in C₆D₆ resulted in a rapid color change to red and the effervescence of dinitrogen. ¹H NMR spectroscopy showed two sets of characteristic Pn ring signals corresponding to **8** and unreacted **1** in approximately equal ratio. Addition of a further 1 equivalent of PhN₃ showed complete conversion to **8** (Scheme 5).

Scheme 5. Summary of synthetic routes to 8. R = Si-ⁱPr₃.



Metal-driven reductive transformations of organic azides to imido complexes are well known for titanium,^{65,71–73} and other early transition metals.^{74–77} However with Ti mononuclear *terminal*-imido complexes are typically formed. The reaction of **1** with PhN₃ can be considered a 2e⁻ redox process per organoazide. The imido [PhN]²⁻

fragment produced is isolobal with O²⁻, and hence this reaction parallels that of **1** with excess N₂O, which yields [(η⁸-Pn⁺)Ti]₂(μ-O)₂.⁷⁸

CONCLUSIONS

This study has expanded the chemistry of the dititanium bis(pentalene) complex **1** towards isocyanides and heteroallenes, which provides useful insights into that with CO and CO₂.

Reaction of **1** with methylisocyanide yields a 1:1 adduct **2**, in which is analogous to the monocarbonyl complex (μ:η⁵,η⁵-Pn⁺)₂Ti₂(μ:η²-CO), but in contrast to the CO chemistry previously reported, excess MeNC does not lead to the formation higher adducts. The thermally stable carbodiimide adduct **3** shows symmetrical binding to the Ti₂ unit that can be seen as another model for the bonding situation in (μ:η⁵,η⁵-Pn⁺)₂Ti₂(CO₂). The reaction of **1** with PhNCO to give unusual phenyl-carbonimide bridged **4** shows that heteroallene reactions can be kinetically stabilized at the Ti(III)–Ti(III) stage, however further studies are required to fully rationalize this transformation. This would also help to clarify the proposed disproportionation step in the reductive activation of CO₂ by **1**.

The reactivity with dichalcogenides and azobenzene shows **1** can act as a 2e⁻ and 4e⁻ reductant respectively. These reactions were clean and essentially quantitative, giving diamagnetic products, which were straightforwardly identified by ¹H NMR spectroscopy. Hence, these studies provide a blueprint for more predictable redox transformations of the [Ti=Ti]⁴⁺ core in **1**, which are consistent with the irreversible oxidation potential measured at –1.06 vs FeCp₂^{+/0}.

The reactivity of **1** invites comparisons with that of the titanocene(II) fragment explored by Floriani and others, and also that of the electron rich di-tungsten hexaalkoxide complexes of Cotton, Chisholm and co-workers. However, the chemistry of titanium–titanium multiple bonds remains relatively unexplored and work is ongoing in our laboratory to provide further examples of their reactivity.

EXPERIMENTAL SECTION

General procedures

All manipulations were carried out using standard Schlenk techniques under Ar, or in an MBraun glovebox under N₂ or Ar. All glassware was dried at 160 °C overnight prior to use. Solvents were purified by pre-drying over sodium wire and then distilled over Na (toluene), K (THF, hexane) or Na–K alloy (Et₂O, pentane) under a N₂ atmosphere. Dried solvents were collected, degassed three times and stored over argon in K mirrored ampoules, except THF and Et₂O which were stored in ampoules containing activated 4 Å molecular sieves. Deuterated solvents (C₆D₆, toluene-*d*₈, cyclohexane-*d*₁₂, methylcyclohexane-*d*₁₄) were purchased from Aldrich, degassed by three freeze–pump–thaw cycles, dried by refluxing over K for 3 days, vacuum distilled into ampoules and

stored under N₂. The starting compound (μ : η^5 , η^5 -Pn⁺)₂Ti₂ was prepared according to published procedures.⁶ Reagents 1,3-*N,N'*-di-*p*-tolylcarbodiimide, azidobenzene (0.5 M solution in Me-THF) and azobenzene were purchased from Aldrich and used as received. Isocyanide PhNCO (Aldrich) was degassed, and stored under argon. Isocyanides MeNC and ^tBuNC were stored over 4 Å sieves and degassed before use. Diphenyl dichalcogenides Ph₂S₂, Ph₂Se₂ and Ph₂Te₂ (Acros) were kindly donated by Prof K. Meyer, FAU Erlangen-Nürnberg. NMR spectra were measured on Varian VNMRs 400 (¹H 399.5 MHz; ¹³C{¹H} 100.25 MHz; ²⁹Si{¹H} 79.4 MHz) or VNMRs 500 (¹H 499.9 MHz; ¹³C{¹H} 125.7 MHz) spectrometers. The spectra were referenced internally to the residual protic solvent (¹H) or the signals of the solvent (¹³C). ⁷⁷Se, ²⁹Si and ¹²⁵Te NMR spectra were referenced relative to Me₂Se, SiMe₄ and Me₂Te (90%) respectively. IR spectra were recorded between NaCl plates using a Perkin-Elmer Spectrum One FTIR instrument. Mass spectra were recorded using a VG Autospec Fisons instrument (EI at 70 eV). Elemental analyses were carried out at the Elemental Analysis Service, London Metropolitan University.

Syntheses

(μ : η^5 , η^5 -Pn⁺)₂Ti₂(μ : η^2 -CNMe) (**2**). A solution of MeNC (32 μ L, 3.1 M in toluene-*d*₈, 0.099 mmol) was added dropwise to a solution of **1** (46 mg, 0.050 mmol) in pentane (1.5 mL) at -35 °C. Following addition, the purple mixture was allowed to warm to room temperature and stir for 20 min. The resultant solution was filtered and concentrated to ca. 0.5 mL and after cooling to -35 °C deposited dark red crystals that were isolated by decantation and dried *in vacuo*. Total yield: 39 mg (81% with respect to **1**). ¹H NMR (toluene-*d*₈, 399.5 MHz, 303 K): δ _H 7.70 (1H, d, ³J_{HH} = 3.4 Hz, Pn H), 7.25 (1H, d, ³J_{HH} = 3.0 Hz, Pn H), 6.55 (1H, d, ³J_{HH} = 3.2 Hz, Pn H), 6.19 (1H, d, ³J_{HH} = 3.3 Hz, Pn H), 6.01 (1H, d, ³J_{HH} = 2.9 Hz, Pn H), 5.96 (1H, d, ³J_{HH} = 3.2 Hz, Pn H), 5.89 (1H, d, ³J_{HH} = 3.5 Hz, Pn H), 5.77 (1H, d, ³J_{HH} = 3.4 Hz, Pn H), 3.25 (3H, s, CNCH₃), 1.48 (6H, m, ⁱPr CH), 1.31 (6H, m, ⁱPr CH), 1.19 (9H, d, ³J_{HH} = 6.4 Hz, ⁱPr CH₃), 1.18 (9H, d, ³J_{HH} = 7.1 Hz, ⁱPr CH₃), 1.17 (9H, d, ³J_{HH} = 6.9 Hz, ⁱPr CH₃), 1.13 (9H, d, ³J_{HH} = 7.3 Hz, ⁱPr CH₃), 1.06 (9H, d, ³J_{HH} = 7.5 Hz, ⁱPr CH₃), 1.03 (9H, d, ³J_{HH} = 7.3 Hz, ⁱPr CH₃), 0.99 (9H, d, ³J_{HH} = 3 Hz, ⁱPr CH₃), 0.97 (9H, d, ³J_{HH} = 7.0 Hz, ⁱPr CH₃). ¹³C{¹H} NMR (toluene-*d*₈, 100.5 MHz, 303 K): δ _C 289.2 (CNCH₃), 132.5 (Pn C), 132.2 (Pn C), 130.5 (Pn C), 126.2 (Pn C), 126.0 (Pn C), 123.2 (Pn C), 111.1 (Pn C), 107.5 (Pn C), 107.0 (Pn C), 106.3 (Pn C), 106.2 (Pn C), 94.78 (Pn C), 94.25 (Pn C), 91.44 (Pn C), 90.81 (Pn C), 44.65 (CNCH₃), 20.46 (ⁱPr CH₃), 20.40 (ⁱPr CH₃), 20.35 (ⁱPr CH₃), 20.27 (ⁱPr CH₃), 20.19 (br, overlapping m, ⁱPr CH₃), 20.09 (ⁱPr CH₃), 19.91 (ⁱPr CH₃), 14.67 (ⁱPr CH), 14.50 (ⁱPr CH), 13.91 (ⁱPr CH), 13.44 (ⁱPr CH). ²⁹Si{¹H} NMR (toluene-*d*₈, 79.4 MHz, 303 K): δ _{Si} 7.92, 7.26, 7.23, 6.25. EI-MS: *m/z* = 967 (25%), [M]⁺; 952 (10%), [M - Me]⁺, 926 (100%), [M - MeNC]⁺. Anal. found (calcd. for C₅₄H₉₅NSi₄Ti₂): C, 66.99 (67.11); H, 10.03 (9.91) %. IR (NaCl): 1642 (ν CN) cm⁻¹.

(μ : η^5 , η^5 -Pn⁺)₂Ti₂(μ -C{N(4-C₆H₄CH₃)₂}) (**3**). Solid 1,3-*N,N'*-di-*p*-tolylcarbodiimide (13 mg, 0.057 mmol) was added slowly to a solution of **1** (53 mg, 0.057 mmol) in

pentane (2 mL) at room temperature, resulting in a color change from deep red to brown-green. The solvent was removed by slow evaporation at ambient pressure and the brown residue was redissolved in SiMe₄ (1 mL). Cooling this solution to -35 °C produced bronze crystals that were isolated by decantation and dried *in vacuo*. Total yield: 60 mg (92% with respect to **1**). ¹H NMR (methylcyclohexane-*d*₁₄, 400.20 MHz, 298 K): δ _H 7.23 (2H, d, ³J_{HH} = 2.8 Hz, Pn H), 7.02 (4H, t, ³J_{HH} = 8.0 Hz, Tol *m*-H), 6.66 (4H, t, ³J_{HH} = 8.0 Hz, Tol *o*-H), 6.57 (2H, d, ³J_{HH} = 3.3 Hz, Pn H), 6.39 (2H, d, ³J_{HH} = 2.7 Hz, Pn H), 6.18 (2H, d, ³J_{HH} = 3.4 Hz, Pn H), 2.36 (2H, s, Tol CH₃), 1.61 (6H, m, ⁱPr CH), 1.23 (18H, d, ³J_{HH} = 7.3 Hz, ⁱPr CH₃), 1.14 (6H, m, ⁱPr CH), 1.11 (18H, d, ³J_{HH} = 7.4 Hz, ⁱPr CH₃), 0.98 (18H, d, ³J_{HH} = 7.3 Hz, ⁱPr CH₃), 0.86 (18H, d, ³J_{HH} = 7.3 Hz, ⁱPr CH₃). ¹³C{¹H} NMR (methylcyclohexane-*d*₁₄, 100.65 MHz, 298 K): δ _C 182.3 (C{NTol}₂), 147.0 (Tol *p*-C), 134.0 (Pn bridgehead C), 132.6 (Tol *i*-C), 132.5 (Pn CH), 129.5 (Tol *o*-C), 129.1 (Pn bridgehead C), 126.6 (Tol *m*-C), 125.4 (Pn CH), 118.7 (Pn CH), 109.4 (Pn CH), 99.00 (Pn C-Si), 93.93 (Pn C-Si), 22.07 (Tol CH₃), 21.05 (ⁱPr CH₃), 21.03 (ⁱPr CH₃), 20.82 (ⁱPr CH₃), 20.67 (ⁱPr CH₃), 15.43, (ⁱPr CH), 13.80 (ⁱPr CH). ²⁹Si{¹H} NMR (methylcyclohexane-*d*₁₄, 99.31 MHz, 298 K): δ _{Si} 3.28, 3.04. EI-MS: *m/z* = 1144–1149 (principal peak 1146, 20%), [M]⁺; 1027–1032 (principal peak 1029, 100%), [M - CN(C₆H₄CH₃)₂]⁺. Anal. found (calcd. for C₆₇H₁₀₆N₂Si₄Ti₂): C, 69.87 (70.12); H, 9.42 (9.31); N, 2.48 (2.44) %. IR (NaCl): 1659 (ν _{asym} NCN), 1599 (ν aromatic C=C), 1318 (ν _{sym} NCN) cm⁻¹.

[(η^8 -Pn⁺)Ti]₂(μ - κ^2 : κ^2 -O₂CNPh) (**4**). To a solution of **1** (70 mg, 0.076 mmol) in pentane (1 mL) was added a solution of PhNCO (9 mg, 0.076 mmol) in pentane (2 mL), dropwise at -35 °C. A color change to brown-green occurred and the mixture was allowed to warm to room temperature, stirred for 10 min and then filtered. The filtrate was concentrated to ca. 1 mL and after cooling to -35 °C, deposited pale green crystals that were isolated by decantation and dried *in vacuo*. Total yield: 32 mg (40% with respect to **1**). ¹H NMR (THF-*d*₈, 399.5 MHz, 303 K): δ _H 7.25 (br, $\Delta\nu_{1/2}$ = 65 Hz, Pn H), 5.96 (br, $\Delta\nu_{1/2}$ = 57 Hz, Pn H), 1.77 (br, $\Delta\nu_{1/2}$ = 110 Hz, ⁱPr CH), 1.37 (br, $\Delta\nu_{1/2}$ = 280 Hz, ⁱPr CH₃). ¹³C and ²⁹Si NMR resonances were not observed due to the paramagnetic nature of **4**. EI-MS: *m/z* = 1059–1062 (principal peak 1060, 15%), [M]⁺; 1031–1035 (principal peak 1032, 20%), [M - CO]⁺; 955–961 (principal peak 957, 100%), [M - PhNC]⁺. Anal. found (calcd. for C₅₉H₉₇NO₂Si₄Ti₂): C, 66.73 (66.82); H, 9.09 (9.22); N, 1.36 (1.32) %. IR (NaCl): 1564 (ν aromatic C=C) cm⁻¹.

(μ : η^5 , η^5 -Pn⁺)₂[Ti(SPh)]₂ (**5**). Solid PhSSPh (21 mg, 0.096 mmol) was added slowly to a stirring solution of **1** (89 mg, 0.096 mmol) in toluene (2 mL) at room temperature, resulting in a color change from deep red to red-brown. The solvent was removed under reduced pressure and the products were extracted with pentane (3 mL) and filtered. The red-brown filtrate was concentrated to ca. 1 mL and after cooling to -35 °C, deposited brown crystals that were isolated by decantation and dried *in vacuo*. Total yield: 82 mg (75% with respect to **1**). ¹H NMR (C₆D₆, 399.5 MHz, 303 K): δ _H 8.34 (2H, d, ³J_{HH} = 3.2 Hz, Pn H), 7.65 (4H, d,

$^3J_{\text{HH}} = 7.2$ Hz, Ph *o*-H), 7.37 (2H, d, $^3J_{\text{HH}} = 3.3$ Hz, Pn H), 7.24 (4H, t, $^3J_{\text{HH}} = 7.7$ Hz, Ph *m*-H), 7.02 (2H, t, $^3J_{\text{HH}} = 7.4$ Hz, Ph *p*-H), 5.60 (2H, d, $^3J_{\text{HH}} = 3.1$ Hz, Pn H), 5.23 (2H, d, $^3J_{\text{HH}} = 3.3$ Hz, Pn H), 1.72 (6H, m, $^1\text{Pr CH}$), 1.64 (6H, m, $^1\text{Pr CH}$), 1.27 (18H, d, $^3J_{\text{HH}} = 7.4$ Hz, $^1\text{Pr CH}_3$), 1.17 (18H, d, $^3J_{\text{HH}} = 7.4$ Hz, $^1\text{Pr CH}_3$), 1.11 (18H, d, $^3J_{\text{HH}} = 7.5$ Hz, $^1\text{Pr CH}_3$), 0.97 (18H, d, $^3J_{\text{HH}} = 7.5$ Hz, $^1\text{Pr CH}_3$). $^{13}\text{C}\{^1\text{H}\}$ NMR (C_6D_6 , 100.5 MHz, 303 K): δ_{C} 152.7 (Ph *i*-C), 142.0 (Pn C), 137.9 (Pn CH), 132.1 (Ph *o*-C), 128.6 (Ph *m*-C), 127.2 (Pn CH), 126.3 (Pn CH), 125.4 (Ph *p*-C), 117.2 (Pn C), 111.2 (Pn CH), 91.90 (Pn C), 20.45 ($^1\text{Pr CH}_3$), 20.34 ($^1\text{Pr CH}_3$), 20.05 ($^1\text{Pr CH}_3$), 19.92 ($^1\text{Pr CH}_3$), 14.41 ($^1\text{Pr CH}$), 13.19 ($^1\text{Pr CH}$). $^{29}\text{Si}\{^1\text{H}\}$ NMR (C_6D_6 , 79.4 MHz, 303 K): δ_{Si} 4.21, 3.09. EI-MS: $m/z = 1142$ – 1147 (principal peak 1143, 30%), $[\text{M}]^+$; 1063–1069 (principal peak 1065, 100%), $[\text{M} - \text{Ph}]^+$. Anal. found (calcd. for $\text{C}_{64}\text{H}_{102}\text{S}_2\text{Si}_4\text{Ti}_2$): C, 67.13 (67.12); H, 9.14 (8.99) %. IR (NaCl): 1620 (br, ν aromatic C=C) cm^{-1} .

$(\mu\text{-}\eta^5\text{-}\eta^5\text{-Pn}^+)_2[\text{Ti}(\text{SePh})_2]$ (**6**). To a solution of **1** (92 mg, 0.099 mmol) in toluene (1 mL) was added a solution of PhSeSePh (31 mg, 0.099 mmol) in toluene (2 mL), dropwise at room temperature. A color change from deep red to brown was observed and the mixture was allowed to stir for 30 min. The solvent was removed under reduced pressure and the products were extracted with pentane (4 mL) and filtered. The red-brown filtrate was concentrated to ca. 2 mL and after cooling to -35°C , deposited red-brown crystals that were isolated by decantation and dried *in vacuo*. Total yield: 106 mg (86% with respect to **1**). Subsequent recrystallization from Et_2O at -35°C afforded X-ray quality crystals. ^1H NMR (cyclohexane- d_{12} , 399.5 MHz, 303 K): δ_{H} 8.08 (2H, d, $^3J_{\text{HH}} = 3.2$ Hz, Pn H), 7.40 (4H, d, $^3J_{\text{HH}} = 7.0$ Hz, Ph *o*-H), 7.27 (2H, d, $^3J_{\text{HH}} = 3.3$ Hz, Pn H), 7.11 (4H, t, $^3J_{\text{HH}} = 7.3$ Hz, Ph *m*-H), 7.04 (2H, t, $^3J_{\text{HH}} = 7.3$ Hz, Ph *p*-H), 5.37 (2H, d, $^3J_{\text{HH}} = 3.1$ Hz, Pn H), 5.04 (2H, d, $^3J_{\text{HH}} = 3.2$ Hz, Pn H), 1.69–1.58 (12H, overlapping m, $^1\text{Pr CH}$), 1.26 (18H, d, $^3J_{\text{HH}} = 7.4$ Hz, $^1\text{Pr CH}_3$), 1.05 (18H, d, $^3J_{\text{HH}} = 7.4$ Hz, $^1\text{Pr CH}_3$), 0.97 (18H, d, $^3J_{\text{HH}} = 7.5$ Hz, $^1\text{Pr CH}_3$), 0.92 (18H, d, $^3J_{\text{HH}} = 7.5$ Hz, $^1\text{Pr CH}_3$). $^{13}\text{C}\{^1\text{H}\}$ NMR (cyclohexane- d_{12} , 100.5 MHz, 303 K): δ_{C} 145.5 (Ph *i*-C), 141.9 (Pn C), 136.9 (Pn CH), 135.2 (Ph *o*-C), 128.7 (Ph *m*-C), 128.6 (Pn CH), 127.5 (Pn CH), 125.8 (Ph *p*-C), 115.7 (Pn C), 111.3 (Pn CH), 91.07 (Pn C), 20.68 ($^1\text{Pr CH}_3$), 20.62 ($^1\text{Pr CH}_3$), 20.30 ($^1\text{Pr CH}_3$), 20.21 ($^1\text{Pr CH}_3$), 15.00 ($^1\text{Pr CH}$), 13.95 ($^1\text{Pr CH}$). $^{77}\text{Se}\{^1\text{H}\}$ NMR (cyclohexane- d_{12} , 76.21 MHz, 303 K): δ_{Se} 511. $^{29}\text{Si}\{^1\text{H}\}$ NMR (cyclohexane- d_{12} , 100.5 MHz, 303 K): δ_{Si} 4.88, 2.77. EI-MS: $m/z = 1237$ (60%), $[\text{M}]^+$. Anal. found (calcd. for $\text{C}_{64}\text{H}_{102}\text{Se}_2\text{Si}_4\text{Ti}_2$): C, 61.97 (62.12); H, 8.35 (8.31) %. IR (NaCl): 1575 (sh, ν aromatic C=C) cm^{-1} .

$(\mu\text{-}\eta^5\text{-}\eta^5\text{-Pn}^+)_2[\text{Ti}(\text{TePh})_2]$ (**7**). To a solution of **1** (88.5 mg, 0.0956 mmol) in toluene (2 mL) was added a solution of PhTeTePh (39.1 mg, 0.0956 mmol) in toluene (2 mL), dropwise at room temperature. A color change from deep red to dark brown was observed and the mixture was allowed to stir for 30 min. The solvent was removed under reduced pressure and the products were extracted with pentane (4 mL) and filtered. The red-brown filtrate was concentrated to ca. 1 mL and after cooling to -35°C , deposited dark brown crystals that were isolated by decantation and dried *in vacuo*. Total yield: 90 mg (71% with re-

spect to **1**). ^1H NMR (cyclohexane- d_{12} , 499.9 MHz, 303 K): δ_{H} 7.95 (2H, d, $^3J_{\text{HH}} = 3.0$ Hz, Pn H), 7.90 (2H, d, $^3J_{\text{HH}} = 3.1$ Hz, Pn H), 7.74 (4H, dd, $J = 2.8, 6.2$ Hz, Ph *o*-H), 7.20–7.16 (6H, overlapping m, Ph *m*- and *p*-H), 5.44 (2H, d, $^3J_{\text{HH}} = 2.9$ Hz, Pn H), 5.31 (2H, d, $^3J_{\text{HH}} = 3.1$ Hz, Pn H), 1.69 (6H, m, $^1\text{Pr CH}$), 1.54 (6H, m, $^1\text{Pr CH}$), 1.23 (18H, d, $^3J_{\text{HH}} = 7.3$ Hz, $^1\text{Pr CH}_3$), 1.04–0.96 (32H, overlapping m, $^1\text{Pr CH}_3$), 0.90 (18H, d, $^3J_{\text{HH}} = 7.5$ Hz, $^1\text{Pr CH}_3$). $^{13}\text{C}\{^1\text{H}\}$ NMR (cyclohexane- d_{12} , 125.7 MHz, 303 K): δ_{C} 141.5 (Ph *o*-C), 139.5 (Pn C), 133.9 (Pn CH), 129.2 (Pn CH), 129.0 (Ph C), 127.1 (Ph C), 126.7 (Pn C), 122.2 (Pn C), 112.4 (Pn CH), 111.0 (Pn C), 92.80 (Pn C), 20.79 ($^1\text{Pr CH}_3$), 20.77 ($^1\text{Pr CH}_3$), 20.26 ($^1\text{Pr CH}_3$), 20.13 ($^1\text{Pr CH}_3$), 15.01–14.90 (overlapping m, $^1\text{Pr CH}$). $^{29}\text{Si}\{^1\text{H}\}$ NMR (cyclohexane- d_{12} , 303 K): δ_{Si} 5.20, 2.74. $^{125}\text{Te}\{^1\text{H}\}$ NMR (cyclohexane- d_{12} , 126.04 MHz, 303 K): δ_{Te} 418. EI-MS: $m/z = 1303$ – 1312 (principal peak 1307, 50%), $[\text{M} - \text{CMe}]^+$; 1174–1183 (principal peak 1179, 80%), $[\text{M} - ^1\text{Pr}]^+$. Anal. found (calcd. for $\text{C}_{64}\text{H}_{102}\text{Te}_2\text{Si}_4\text{Ti}_2$): C, 57.60 (57.59); H, 7.69 (7.70) %. IR (NaCl): 2193, 2092, 1572 (sh, ν aromatic C=C) cm^{-1} .

$[(\eta^8\text{-Pn}^+)\text{Ti}]_2(\mu\text{-NPh})_2$ (**8**). METHOD A: To a solution of **1** (87 mg, 0.094 mmol) in toluene (2 mL) was added a solution of azobenzene (17 mg, 0.094 mmol) in toluene (2 mL), dropwise at room temperature. A color change to dark red was observed and the mixture was allowed to stir for 30 min. The solvent was removed under reduced pressure and the products were extracted with hexane (2 mL) and filtered. The red filtrate was concentrated to ca. 1 mL and after cooling to -35°C , deposited red crystals that were isolated by decantation and dried *in vacuo*. Total yield: 73 mg (70% with respect to **1**). METHOD B: To a solution of **1** (15 mg, 0.016 mmol) in pentane (3 mL) at -35°C was added azidobenzene (32 μL , 0.016 mmol, 0.5 M soln in Me-THF), dropwise. Effervescence and a color change to red was observed, and the reaction mixture was allowed to warm to room temperature and stir for 10 mins. The solvent was removed *in vacuo* and ^1H NMR spectroscopy showed ca. 50% conversion of **1** to **8**. Addition of further azidobenzene (32 μL , 0.016 mmol, 0.5 M soln in Me-THF) to the reaction mixture furnished **8** in essentially quantitative yield. ^1H NMR (C_6D_6 , 399.5 MHz, 303 K): δ_{H} 6.98 (4H, t, $^3J_{\text{HH}} = 7.8$ Hz, Ph *m*-H), 6.71 (4H, d, $^3J_{\text{HH}} = 3.2$ Hz, Pn H), 6.62 (2H, t, $^3J_{\text{HH}} = 7.3$ Hz, Ph *p*-H), 6.42 (4H, d, $^3J_{\text{HH}} = 7.3$ Hz, Ph *o*-H), 5.22 (4H, d, $^3J_{\text{HH}} = 3.2$ Hz, Pn H), 1.15 (36H, d, $^3J_{\text{HH}} = 7.5$ Hz, $^1\text{Pr CH}_3$), 1.13 (36H, d, $^3J_{\text{HH}} = 7.6$ Hz, $^1\text{Pr CH}_3$), 0.93 (12H, m, $^1\text{Pr CH}$). $^{13}\text{C}\{^1\text{H}\}$ NMR (C_6D_6 , 100.5 MHz, 303 K): δ_{C} 167.3 (Ph *i*-C), 149.0 (Pn bridgehead C), 134.0 (Pn CH), 127.3 (Ph *m*-C), 120.6 (Ph *p*-C), 119.8 (Ph *o*-C), 114.4 (Pn CH), 111.4 (Pn C-Si), 20.01 ($^1\text{Pr CH}_3$), 19.87 ($^1\text{Pr CH}_3$), 12.78 ($^1\text{Pr CH}$). $^{29}\text{Si}\{^1\text{H}\}$ NMR (C_6D_6 , 100.5 MHz, 303 K): δ_{Si} 0.61. EI-MS: $m/z = 1104$ – 1111 (principal peak 1107, 100%), $[\text{M}]^+$; 1030–1034 (principal peak 1032, 30%), $[\text{M} - \text{Ph}]^+$. Anal. found (calcd. for $\text{C}_{64}\text{H}_{102}\text{N}_2\text{Si}_4\text{Ti}_2$): C, 67.13 (67.12); H, 9.14 (8.99) %. IR (NaCl): 1581 (ν aromatic C=C) cm^{-1} .

X-ray crystallography

Single crystal XRD data for **2**, **4**, **5**, **6** and **8** were collected by the UK National Crystallography Service (NCS),⁷⁹ at the University of Southampton on a Rigaku FR-E+ Ultra High Flux diffractometer ($\lambda_{\text{Mo(K}\alpha)}$) equipped with VariMax

VHF optics and a Saturn 724+ CCD area detector. The data were collected at 100 or 150 K using an Oxford Cryosystems Cobra low temperature device. An empirical absorption correction was carried out using the MULTI-SCAN program.^{80,81} Single crystal XRD data for **3** were collected by the NCS at the Diamond Light Source using synchrotron radiation ($\lambda_{\text{Mo(K}\alpha)}$). An empirical absorption correction was carried out using the 'DTABSCOR' program. Data collected by the NCS were processed using CrystalClear-SM Expert 3.1 b18,⁸² and unit cell parameters were refined against all data. Single crystal XRD data for **5** and **7** were collected at the University of Sussex on a Enraf-Nonius CAD4 diffractometer with graphite-monochromated ($\lambda_{\text{Mo(K}\alpha)}$) radiation or an Agilent Technologies Xcalibur Gemini ultra diffractometer ($\lambda_{\text{Mo(K}\alpha)}$ or $\lambda_{\text{Cu(K}\alpha)}$ source) equipped with a Eos CCD area detector. The data were collected at 173 K using an Oxford Cryosystems Cobra low temperature device. Data were processed using KappaCCD software or CrysAlisPro (version 1.171.36.32),⁸³ and unit cell parameters were refined against all data. An empirical absorption correction was carried out using the MULTI-SCAN program.^{80,81} All structures were solved using SHELXL-2013,⁸⁴ DIRDIF-2008⁸⁵ or SUPERFLIP⁸⁶ and refined on F_o^2 by full-matrix least-squares refinements using SHELXL-2013.⁸⁴ Solutions and refinements were performed using the OLEX2⁸⁷ or WinGX⁸⁸ packages and software packages within. All non-hydrogen atoms were refined with anisotropic displacement parameters. All hydrogen atoms were refined using a riding model. Disordered solvent molecules in **5** and **7** could not be modelled properly; therefore, this disorder was treated by using the SQUEEZE⁸⁹ routine in PLATON.⁹⁰ The solid state structures of **2** and **4** display positional disorder in the MeNC and SiⁱPr groups respectively, and suffer relatively high wR_2 values. This does not effect the key metrical parameters around the metal centers.

Computational details

Density functional calculations were carried using the Amsterdam Density Functional package (version ADF2012.01 and ADF2014.01).⁹¹ The Slater-type orbital (STO) basis sets were of triple- ζ quality augmented with a one polarization function (ADF basis TZP). Core electrons were frozen (C 1s; Ti 2p) in the model of the electronic configuration for each atom. The local density approximation (LDA) by Vosko, Wilk and Nusair (VWN)⁹² was used together with the exchange correlation corrections of Becke and Perdew (BP86).^{93,94}

SUPPORTING INFORMATION

Tables of crystallographic data, additional NMR spectroscopic and computational data, a text file of computed molecule Cartesian coordinates for all structures in .xyz format for convenient visualization; crystallographic data for **2–7** in CIF format. The Supporting Information is available free of charge on the ACS publications website at DOI:

AUTHOR INFORMATION

Corresponding Author

*Email: f.g.cloke@sussex.ac.uk.

Author Contributions

The manuscript was written through contributions of all authors.

Notes

The authors declare no competing financial interest.

ACKNOWLEDGMENTS

We thank the ERC (Project 247390), the EPSRC (EP/M023885/1) and the University of Sussex for financial support. The UK National Crystallography Service (NCS) Southampton is thanked for their assistance with single crystal X-ray data collection. Mr C. J. Inman, Dr N. Tsoureas and Dr I. R. Crossley (Sussex) are thanked for their assistance in the preparation of this manuscript.

REFERENCES

- (1) Cotton, F. A.; Murillo, C. A.; Walton, R. A. *Multiple Bonds Between Metal Atoms*, 3rd ed.; Walton, R. A., Ed.; Clarendon Press, 2005.
- (2) Thomas, C. M. *Comments Inorg. Chem.* 2011, 32 (1), 14–38.
- (3) Krogman, J. P.; Thomas, C. M. *Chem. Commun.* 2014, 50 (40), 5115.
- (4) Walker, W. K.; Kay, B. M.; Michaelis, S. A.; Anderson, D. L.; Smith, S. J.; Ess, D. H.; Michaelis, D. J. *J. Am. Chem. Soc.* 2015, 137 (23), 7371–7378.
- (5) Gade, L. H. In *Molecular Metal-Metal Bonds. Compounds, Synthesis, Properties.*; Liddle, S. T., Ed.; Wiley-VCH, 2015; pp 73–89.
- (6) Kilpatrick, A. F. R.; Green, J. C.; Cloke, F. G. N.; Tsoureas, N. *Chem. Commun.* 2013, 49 (82), 9434–9436.
- (7) Katz, T. J.; Acton, N.; McGinnis, J. *J. Am. Chem. Soc.* 1972, 94 (17), 6205–6206.
- (8) Kuchta, M.; Cloke, F. G. N. *Organometallics* 1998, 17 (10), 1934–1936.
- (9) Balazs, G.; Cloke, F. G. N.; Harrison, A.; Hitchcock, P. B.; Green, J.; Summerscales, O. T. *Chem. Commun.* 2007, 873–875.
- (10) Balazs, G.; Cloke, F. G. N.; Gagliardi, L.; Green, J. C.; Harrison, A.; Hitchcock, P. B.; Shahi, A. R. M.; Summerscales, O. T. *Organometallics* 2008, 27 (9), 2013–2020.
- (11) Ashley, A. E.; Cooper, R. T.; Wildgoose, G. G.; Green, J. C.; O'Hare, D. *J. Am. Chem. Soc.* 2008, 130 (46), 15662–15677.
- (12) Summerscales, O. T.; Rivers, C. J.; Taylor, M. J.; Hitchcock, P. B.; Green, J. C.; Cloke, F. G. N. *Organometallics* 2012, 31 (24), 8613–8617.
- (13) Kilpatrick, A. F. R.; Cloke, F. G. N. *Chem. Commun.* 2014, 50, 2769–2771.
- (14) Kilpatrick, A. F. R.; Green, J. C.; Cloke, F. G. N. *Organometallics* 2015, 34 (20), 4816–4829.
- (15) Mironov, M. A. In *Isocyanide Chemistry: Applications in Synthesis and Material Science*; Nenajdenko, V., Ed.; Wiley VCH, 2012; pp 35–74.
- (16) Stephany, R. W.; de Bie, M. J. A.; Drenth, W. *Org. Magn. Reson.* 1974, 6 (1), 45–47.

- (17) Kilpatrick, A. F. R.; Green, J. C.; Cloke, F. G. N. *Organometallics* 2015, 34 (20), 4830–4843.
- (18) Ramozzi, R.; Chéron, N.; Braïda, B.; Hiberty, P. C.; Fleurat-Lessard, P. *New J. Chem.* 2012, 36 (5), 1137.
- (19) Lindemann, H.; Wiegrebe, L. *Ber. Dtsch. Chem. Ges.* 1930, 63 (7), 1650–1657.
- (20) Yamamoto, Y. *Coord. Chem. Rev.* 1980, 32 (3), 193–233.
- (21) Chisholm, M. H.; Clark, D. L.; Ho, D.; Huffman, J. C. *Organometallics* 1987, 6 (7), 1532–1542.
- (22) Werner, H. *Coord. Chem. Rev.* 1982, 43 (0), 165–185.
- (23) Reichen, W. *Chem. Rev.* 1978, 78 (5), 569–588.
- (24) Bottrill, M.; Gavens, P. D.; McMeeking, J. In *Comprehensive Organometallic Chemistry*; Wilkinson, G., Stone, F. G. A., Abel, E. W., Eds.; Pergamon Press, 1982; Vol. 3.
- (25) Chirik, P. J.; Bouwkamp, M. W. In *Comprehensive Organometallic Chemistry III*; Mingos, D. M. P., Crabtree, R. H., Eds.; Elsevier, 2007; pp 243–279.
- (26) Pyykkö, P.; Atsumi, M. *Chem.–Eur. J.* 2009, 15 (46), 12770–12779.
- (27) Theilmann, O.; Ruhmann, M.; Villinger, A.; Schulz, A.; Seidel, W. W.; Kaleta, K.; Beweries, T.; Arndt, P.; Rosenthal, U. *Angew. Chem. Int. Ed. Engl.* 2010, 49 (48), 9282–9285.
- (28) Romain, C.; Brelot, L.; Bellemin-Lapponnaz, S.; Dargorne, S. *Organometallics* 2010, 29 (5), 1191–1198.
- (29) Li, J.; Schulzke, C.; Merkel, S.; Roesky, H. W.; Samuel, P. P.; Döring, A.; Stalke, D. Z. *Anorg. Allg. Chem.* 2010, 636 (3–4), 511–514.
- (30) Schrock, R. R. *Chem. Rev.* 2002, 102 (1), 145–179.
- (31) Lukens, W. W.; Smith, M. R.; Andersen, R. A. *J. Am. Chem. Soc.* 1996, 118 (7), 1719–1728.
- (32) Brady, E.; Telford, J. R.; Mitchell, G.; Lukens, W. *Acta Crystallogr., Sect. C: Cryst. Struct. Commun.* 1995, 51 (4), 558–560.
- (33) Feldman, J.; Calabrese, J. C. *J. Chem. Soc., Chem. Commun.* 1991, No. 15, 1042–1044.
- (34) De Boer, E. J. M.; Teuben, J. H. J. *Organomet. Chem.* 1979, 166, 193–198.
- (35) Vincent, A. T.; Wheatley, P. J. *J. Chem. Soc., Perkin Trans. 2* 1972, No. 5, 687.
- (36) Darwish, W.; Seikel, E.; Käsmarker, R.; Harms, K.; Sundermeyer, J. *Dalton Trans.* 2011, 40 (8), 1787–1794.
- (37) Cotton, F. A.; Schwotzer, W.; Shamsoum, E. S. *Organometallics* 1985, 4 (3), 461–465.
- (38) Budzichowski, T. A.; Chisholm, M. H.; Folting, K.; Huffman, J. C. *Polyhedron* 1998, 17 (5–6), 857–867.
- (39) Braunstein, P.; Nobel, D. *Chem. Rev.* 1989, 89 (8), 1927–1945.
- (40) Allen, F. H.; Kennard, O.; Watson, D. G.; Brammer, L. *J. Chem. Soc., Perkin Trans. 2* 1987, S1–S19.
- (41) Evans, W. J.; Fujimoto, C. H.; Ziller, J. W. *Organometallics* 2001, 20 (22), 4529–4536.
- (42) Zhang, C.; Liu, R.; Zhang, J.; Chen, Z.; Zhou, X. *Inorg. Chem.* 2006, 45 (15), 5867–5877.
- (43) Patai, S. *Chemistry of Cyanates and Their Thio Derivatives*; J. Wiley, 1977.
- (44) Fachinetti, G.; Floriani, C. *J. Chem. Soc., Dalton Trans.* 1974, No. 22, 2433–2436.
- (45) Howard, W. A.; Trnka, T. M.; Parkin, G. *Inorg. Chem.* 1995, 34, 5900–5909.
- (46) Christou, V.; Arnold, J. *J. Am. Chem. Soc.* 1992, 114 (15), 6240–6242.
- (47) Stephan, D. W.; Nadasdi, T. T. *Coord. Chem. Rev.* 1996, 147, 147–208.
- (48) Klapötke, T. M. *Phosphorus, Sulfur Silicon Relat. Elem.* 1989, 41 (1–2), 105–111.
- (49) Hector, A. L.; Levason, W.; Reid, G.; Reid, S. D.; Webster, M. *Chem. Mater.* 2008, 20 (15), 5100–5106.
- (50) Gerlach, C. P.; Christou, V.; Arnold, J. *Inorg. Chem.* 1996, 35 (10), 2758–2766.
- (51) Christou, V.; Wuller, S. P.; Arnold, J. *J. Am. Chem. Soc.* 1993, 115 (23), 10545–10552.
- (52) Gindelberger, D. E.; Arnold, J. 1994, 13 (11), 4462–4468.
- (53) Cummins, C. C.; Schaller, C. P.; Van Duyne, G. D.; Wolczanski, P. T.; Chan, A. W. E.; Hoffmann, R. *J. Am. Chem. Soc.* 1991, 113 (8), 2985–2994.
- (54) Pyykkö, P.; Atsumi, M. *Chem.–Eur. J.* 2009, 15 (1), 186–197.
- (55) Fischer, J. M.; Piers, W. E.; Macgillivray, L. R.; Zaworotko, M. J. *Inorg. Chem.* 1995, 34 (10), 2499–2500.
- (56) Green, M. J. *Organomet. Chem.* 1995, 500 (1), 127–148.
- (57) Sutton, D. *Chem. Rev.* 1993, 93 (3), 995–1022.
- (58) Fachinetti, G.; Fochi, G.; Floriani, C. *J. Organomet. Chem.* 1973, 57 (2), C51–C54.
- (59) Bart, J.; Bassi, I. W.; Cerruti, G. F.; Calcaterra, M. *Gazz. Chim. Ital.* 1980, 110 (7–8), 423–442.
- (60) Fochi, G.; Floriani, C.; Bart, J.; Giunchi, G. *J. Chem. Soc., Dalton Trans.* 1983, No. 8, 1515–1521.
- (61) Theilmann, O.; Saak, W.; Haase, D.; Beckhaus, R. *Organometallics* 2009, 28 (9), 2799–2807.
- (62) Hill, J. E.; Profilet, R. D.; Fanwick, P. E.; Rothwell, I. P. *Angew. Chem. Int. Ed. Engl.* 1990, 29 (6), 664–665.
- (63) Hill, J. E.; Fanwick, P. E.; Rothwell, I. P. *Inorg. Chem.* 1991, 30, 1143–1144.
- (64) Duchateau, R.; Williams, A. J.; Gambarotta, S.; Chiang, M. Y. *Inorg. Chem.* 1991, 30 (25), 4863–4866.
- (65) Gray, S. D.; Thorman, J. L.; Berreau, L. M.; Woo, L. K. *Inorg. Chem.* 1997, 36 (3), 278–283.
- (66) Gray, S. D.; Thorman, J. L.; Adamian, V. A.; Kadish, K. M.; Woo, L. K. *Inorg. Chem.* 1998, 37 (1), 1–4.
- (67) Gambarotta, S.; Floriani, C.; Chiesi-Villa, A.; Guastini, C. *J. Am. Chem. Soc.* 1983, 105 (25), 7295–7301.
- (68) Grigsby, W. J.; Olmstead, M. M.; Power, P. P. *J. Organomet. Chem.* 1996, 513, 173–180.
- (69) Dunn, S. C.; Hazari, N.; Cowley, A. R.; Green, J. C.; Mountford, P. *Organometallics* 2006, 25 (7), 1755–1770.
- (70) Thorn, D. L.; Nugent, W. A.; Harlow, R. L. *J. Am. Chem. Soc.* 1981, 103, 357–363.
- (71) Mullins, S. M.; Duncan, A. P.; Bergman, R. G.; Arnold, J. *Inorg. Chem.* 2001, 40 (27), 6952–6963.
- (72) Hanna, T. E.; Keresztes, I.; Lobkovsky, E.; Bernskoetter, W. H.; Chirik, P. J. *Organometallics* 2004, 23 (14), 3448–3458.
- (73) Fout, A. R.; Kilgore, U. J.; Mindiola, D. J. *Chem.–Eur. J.* 2007, 13 (34), 9428–9440.
- (74) Wigley, D. E. *Prog. Inorg. Chem.* 1994, 42, 239–482.
- (75) Fickes, M. G.; Davis, W. M.; Cummins, C. C. *J. Am. Chem. Soc.* 1995, 117 (23), 6384–6385.
- (76) Tomson, N. C.; Arnold, J.; Bergman, R. G. *Organometallics* 2010, 29 (21), 5010–5025.
- (77) Obenhuber, A. H.; Gianetti, T. L.; Berrebi, X.; Bergman, R. G.; Arnold, J. *J. Am. Chem. Soc.* 2014, 136, 2994–2997.
- (78) Nugent, W. A.; Mayer, J. M. *Metal-Ligand Multiple Bonds*; Wiley, 1988.
- (79) Coles, S. J.; Gale, P. A. *Chem. Sci.* 2012, 3 (3), 683–689.
- (80) Blessing, R. H.; Langs, D. A. *J. Appl. Crystallogr.* 1987, 20 (5), 427–428.
- (81) Blessing, R. H. *Acta Crystallogr., A, Found. Crystallogr.* 1995, 51, 33–38.
- (82) Rigaku. *CrystalClear* 2011.
- (83) Agilent Technologies. *CrysAlisPro 1.171.36.32* 2011.

- (84) Sheldrick, G. M. *Acta Crystallogr., A, Found. Crystallogr.* 2008, 64 (1), 112–122.
- (85) Beurskens, P. T.; Beurskens, G.; Gelder, R.; Smits, J. M. M.; Garcia-Granda, S.; Gould, R. O. University of Nijmegen, The Netherlands 2008.
- (86) Palatinus, L.; Chapuis, G. *J. Appl. Crystallogr.* 2007, 40 (4), 786–790.
- (87) Dolomanov, O. V.; Bourhis, L. J.; Gildea, R. J.; Howard, J. A. K.; Puschmann, H. *J. Appl. Crystallogr.* 2009, 42 (2), 339–341.
- (88) Farrugia, L. J. *J. Appl. Crystallogr.* 1999, 32 (4), 837–838.
- (89) van der Sluis, P.; Spek, A. L. *Acta Crystallogr., A, Found. Crystallogr.* 1990, 46 (3), 194–201.
- (90) Spek, A. L. *J. Appl. Crystallogr.* 2003, 36 (1), 7–13.
- (91) SCM. *Amsterdam Density Functional, ADF* 2006.
- (92) Vosko, S. H.; Wilk, L.; Nusair, M. *Can. J. Phys.* 1980, 58, 1200–1211.
- (93) Becke, A. *Phys. Rev., A* 1988, 38 (6), 3098–3100.
- (94) Perdew, J. P. *Phys. Rev. B* 1986, 33 (12), 8822–8824.

